JOC*Article*

Synthesis and Characterization of *p*-Phenylenediamine Derivatives Bearing an Electron-Acceptor Unit

Hidehiro Sakurai, Mendra T. S. Ritonga, Harumi Shibatani, and Toshikazu Hirao*

Department of Applied Chemistry, Graduate School of Engineering, Osaka University, Yamada-oka, Suita, Osaka 567-0871, Japan

hirao@chem.eng.osaka-u.ac.jp

Received September 22, 2004

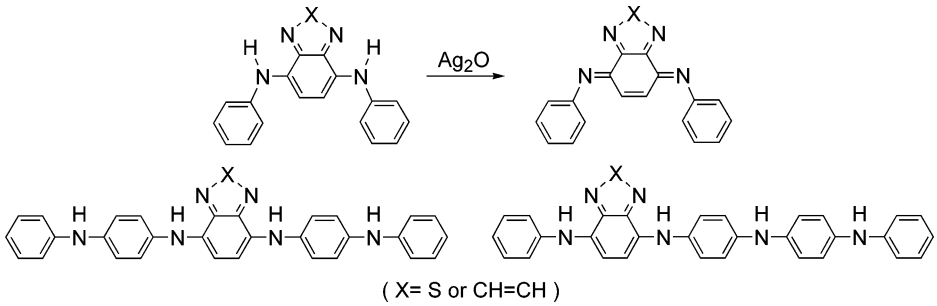

Two series of aniline oligomers bearing fused heterocycles as an electron-acceptor unit were synthesized. They consist of aniline or its derivatives as an electron donor and benzothiadiazole (BT) or quinoxaline (QX) as an electron-acceptor unit. Benzothiadiazoles **1**−**3** were synthesized by palladium-catalyzed amination. Quinoxalines **4**−**6** were prepared by palladium-catalyzed amination or transformation from the benzothiadiazoles. These compounds showed a HOMO−LUMO gap smaller than those of their analogues such as thiophene-substituted BT/QXs. Cyclic voltammetry revealed that the electrochemical behavior is dependent on the position of the acceptor heterocycle. Chemical oxidation with Ag_2O afforded the corresponding 1,4-quinonediimine derivatives as an *E*,*E*-isomer, stereoselectively. As for the BT pentamer analogues **2** and **3**, the first oxidation selectively occurred at the amino group adjacent to the benzothiadiazole unit, giving the regiospecific half-oxidized derivatives. Furthermore, the fully oxidized derivative **24** was isolated and characterized.

Introduction

The π-conjugated polymers have attracted much attention in the application to electrical materials depending on their electrical properties. Among π-conjugated polymers, polyanilines are particularly attractive as a result of their excellent electrical properties and stability.[1] Extensive investigation has provided useful materials such as batteries,[2] light-emitting diodes,[3] antistatic packaging and coatings,[4] microelectronic devices,[5] electrochemical chromatography,[6] and corrosion inhibitors to protect semiconductors or metals.[7] Polyanilines exist in three different discrete redox forms, which include the fully reduced leucoemeraldine base (LE), the semioxidized emeraldine base (EB), and the fully oxidized pernigraniline base (PE) as shown in Scheme 1.[8] The oxidation states of the π-conjugated polymers and oligomers interconvert each other,[9] permitting the construction of a catalytic system for oxidation reactions. Polyanilines serve as synthetic metal catalysts under an oxygen atmosphere in the dehydrogenative oxidation of benzylamines, 2-phenylglycine, and 2,6-di-*t*-butylphenol.[10] Similar catalysis is also performed with the quinonediimine derivatives.[11] The quinonediimine moiety of

(1) (a) Nakajima, T.; Kawagoe, T. *Synth. Met.* **1989**, *28*, C629. (b) Bergeron, J.-Y.; Dao, L. H. *Macromolecules* **1992**, *25*, 3332.
(2) (a) Kitani, A.; Kaya, M.; Sakaki, K. *J. Electrochem. Soc.* **1986**, *133*, 1069. (b) MacDiarmid, A. G.; Yang, L. S.; Huang, W. S.; Humphrey, B. D. *Synth. Met.* **1987**, *18*, 393.
(3) Gustafsson, G.; Cao, Y.; Treacy, G. M.; Klavetter, F.; Colaneri, N.; Heeger, A. G. *Nature* **1992**, *356*, 47.
(4) DeBerry, D. *J. Electrochem. Soc.* **1985**, *132*, 1022.
(5) (a) Genies, E. M.; Lapkowski, M.; Santier, C.; Vieil, E. *Synth. Met*. **1987**, *18*, 631. (b) Nguyen, M. T.; Dao, L. H. *J. Electrochem. Soc.* **1989**, *136*, 2131. (c) Paul, E. W.; Ricco, A. J.; Wrighton, M. S. *J. Phys. Chem.* **1985**, *89*, 1441.
(6) Nagaoka, T.; Kakuno, K.; Fujimoto, M.; Nakao, H.; Yano, J.; Ogura, K. *J. Electroanal. Chem.* **1994**, *368*, 315.
(7) Noufi, R.; Nozik, A. J.; White, J.; Warren, L. F. *J. Electrochem. Soc.* **1982**, *129*, 2261.
(8) Epstein, A. J.; Ginder, J. M., Ritcher, A. F.; MacDiarmid, A. G. In *Conducting Polymers*; Alcacer, L., Ed.; Reidel: Holland, 1987; p 121.
(9) Kaplan, S.; Conwell, E. M.; Richter, A. F.; MacDiarmid, A. G. *Synth. Met.* **1989**, *29*, E235.

10.1021/jo048324j CCC: $30.25
Published on Web 03/09/2005

SCHEME 1. Redox Process of Polyaniline

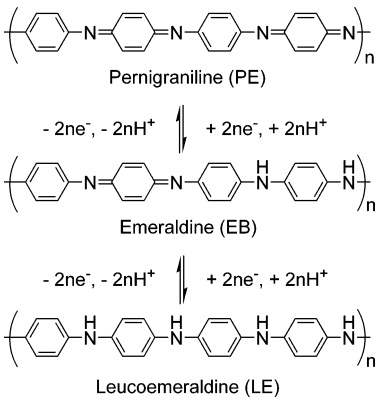

the emeraldine base has been revealed to be capable of participating in the complexation with transition metals.[12]

Band gap control of π-conjugated polymers is a research issue of ongoing interest. Controlling the band gap may give a polymer with the desired electrical and optical properties, and reduction of the band gap to approximately zero is expected to afford a conducting polymer.[13] The synthetic principles for lowering the band gap of linear conjugated polymers have been reviewed by Roncali.[14] One successful and potentially versatile strategy to achieve low-band-gap conjugated polymers follows the pioneering work of Havinga[15] and involves the alternation of electron-rich (donor, D) and electron-deficient (acceptor, A) units in the π-conjugated polymer chain. In recent years, electrochemical polymerization has been employed to prepare polymers consisting of an electron-withdrawing moiety such as 2,1,3-benzothiadiazole, thieno-[3,4-*b*]pyrazine, or [1,2,5]thiadiazolo[3,4-*g*]quinoxaline, and an electron-releasing bithiophene or *N*,*N*′-dimethylbipyrrole. The poly(D−A) systems exhibit optical band gaps as low as 0.5 eV.[16] An extremely narrow optical band gap of 0.3 eV was recently reported for an electrogenerated polymer derived from a bithiophenic precursor involving thieno[3,4-*b*]pyrazine and 3,4-ethylenedioxythiophene.[17] The application of π-conjugated systems to the fields of electronic and photonic devices, however, requires solution-processible materials, and hence the use of electrochemical polymerization is not straightforward. Within the class of low-band-gap alternating D−A polymers, solution-processible materials are scarce and only a precursor polymer based on pyrrole and 2,1,3-benzothiadiazole has been reported.[18] In our design of low-band-gap conjugated systems for application to material devices and complexation with transition metals, the use of a moderately strong acceptor that bears coordination sites is required. 2,1,3-Benzothiadiazole[18,19] and quinoxaline,[20] which bear two electron-withdrawing imine (C=N) nitrogens, are known as typical electron-accepting units. When these units are combined with electron-donating units, the donor−acceptor polymers or oligomers may exhibit low band gap. However, most of these donor−acceptor polymers comprise pyrrole, thiophene, or phenylene as a donor unit. Introduction of acceptor units such as benzothiadiazole or quinoxaline into an aniline oligomer chain is expected to give novel π-conjugated compounds that exhibit different redox properties as compared with those of aniline oligomers.[5] In this paper, we report the synthesis and characterization of *p*-phenylenediamine derivatives bearing a benzothiadiazole or quinoxaline unit. Not only **1** or **4** but also the longer derivatives **2** and **3** bearing the benzothiadiazole unit or **5** and **6** bearing the quinoxaline unit in a different position (Figure 1) were synthesized and characterized in order to study the position effect of the acceptor unit in the aniline oligomer chain.[21]

Results and Discussion

1. Synthesis of 1−6. *p*-Phenylenediamine derivatives **1**, **2**, and **3** bearing a benzothiadiazole unit were prepared as shown in Scheme 2. Amination of 4,7-dibromo-2,1,3-benzothiadiazole (**7**)[22] was carried out by modifying a method reported for the preparation of aniline oligomers by Buchwald et al.[23] Palladium-catalyzed amination of **7** with aniline (**8**) using bis(2-(diphenylphosphino)phenyl) ether (DPEphos)[24] as a ligand in refluxing toluene afforded the bis-coupled product **1** in 91% yield. The reaction of **7** with *N*-phenyl-1,4-phenylenediamine (**9**) also gave **2** in 55% yield. For the preparation of unsym-

(10) (a) Hirao, T.; Higuchi, M.; Ikeda, I.; Oshiro, Y. *J. Chem. Soc., Chem. Commun.* **1993**, 194. (b) Hirao, T.; Higuchi, M.; Oshiro, Y.; Ikeda, I. *Chem. Lett.* **1993**, 1889. (c) Higuchi, M.; Ikeda, I.; Hirao, T. *J. Org. Chem.* **1997**, *62*, 1072.

(11) Hirao, T.; Fukuhara, S. *J. Org. Chem.* **1998**, *63*, 7534.

(12) (a) Higuchi, M.; Yamaguchi, S.; Hirao, T. *Synlett* **1996**, 1213. (b) Higuchi, M.; Imoda, D.; Hirao, T. *Macromolecules* **1996**, *29*, 8277. (c) Hirao, T.; Yamaguchi, S.; Fukuhara, S. *Tetrahedron Lett.* **1999**, *40*, 3009. (d) Hirao, T.; Yamaguchi, S.; Fukuhara, S. *Synth. Met.* **1999**, *106*, 67. (e) Moriuchi, T.; Bandoh, S.; Miyaishi, M.; Hirao, T. *Eur. J. Inorg. Chem.* **2001**, 651. (f) Hirao, T.; Fukuhara, S.; Otomaru, Y.; Moriuchi, T. *Synth. Met.* **2001**, *123*, 373.

(13) (a) Bredas, J. L.; Heeger, A. J.; Wudl, F. *J. Chem. Phys.* **1986**, *85*, 4673. (b) Bredas, J. L. *Synth. Met.* **1987**, *17*, 115.

(14) Roncali, J. *Chem. Rev.* **1997**, *97*, 173.

(15) (a) Havinga, E. E.; ten Hoeve, W.; Wynberg, H. *Polym. Bull.* **1992**, *29*, 119. (b) Havinga, E. E.; ten Hoeve, W.; Wynberg, H. *Synth. Met.* **1993**, *55*, 299.

(16) (a) Karikomi, M.; Kitamura, C.; Tanaka, S.; Yamashita, Y. *J. Am. Chem. Soc.* **1995**, *117*, 6791. (b) Kitamura, C.; Tanaka, S.; Yamashita, Y. *Chem. Mater.* **1996**, *8*, 570.

(17) Akoudad, S.; Roncali, J. *Chem. Commun.* **1998**, 2081.

(18) van Mullekom, H. A. M.; Vekemans, J. A. J. M.; Meijer, E. W. *Chem. Commun.* **1996**, 2163.

(19) (a) Yamashita, Y.; Ono, K.; Tomura, M.; Tanaka, S. *Tetrahedron* **1997**, *53*, 10169. (b) van Mullekom, H. A. M.; Vekemans, J. A. J. M.; Meijer, E. W. *Chem. Eur. J.* **1998**, *4*, 1235. (c) Raimundo, J. M.; Blanchard, P.; Brisset, H.; Akoudad, S.; Roncali, J. *Chem. Commun.* **2000**, 939. (d) Morikita, T.; Yamaguchi, I.; Yamamoto, T. *Adv. Mater.* **2001**, *13*, 1862. (e) Jayakannan, M.; van Hal, P. A.; Janssen, R. A. J. *J. Polym. Sci. A* **2002**, *40*, 2360. (f) Kitamura, C.; Saito, K.; Nakagawa, M.; Ouchi, M.; Yoneda, A.; Yamashita, Y. *Tetrahedron Lett.* **2002**, *43*, 3373.

(20) (a) Yamamoto, T.; Maruyama, T.; Zhou, Z.-H.; Ito, T.; Fukuda, T.; Yoneda, Y.; Begum, F.; Ikeda, T.; Sasaki, S.; Takezoe, H.; Fukuda, A.; Kubota, K. *J. Am. Chem. Soc.* **1994**, *116*, 4832. (b) Yamamoto, T.; Kanbara, T.; Ooba, N.; Tomaru, S. *Chem. Lett.* **1994**, 1709. (c) Yamamoto, T.; Zhou, Z.-H.; Kanbara, T.; Shimura, M.; Kizu, K.; Maruyama, T.; Nakamura, Y.; Fukuda, T.; Lee, B.-L.; Ooba, N.; Tomaru, S.; Kurihara, T.; Kaino, T.; Kubota, K.; Sasaki, S. *J. Am. Chem. Soc.* **1996**, *118*, 10389.

(21) Preliminary results have been reported. See: (a) Ritonga, M. T. S.; Sakurai, H.; Hirao, T. *Tetrahedron Lett.* **2002**, *43*, 9009. (b) Hirao, T.; Sakurai, H.; Ritonga, M. T. S. *Proc. Electrochem. Soc.* **2003**, *12*, 189.

(22) Pilgram, K.; Zupan, M.; Skiles, R. *J. Heterocycl. Chem.* **1970**, *7*, 629.

(23) Sadighi, J. P.; Singer, R. A.; Buchwald, S. L. *J. Am. Chem. Soc.* **1998**, *120*, 4960.

(24) Kranenburg, M.; van der Burgt, Y. E. M.; Kamer, P. C. J.; van Leeuwen, P. W. N. M.; Goublitz, K.; Fraanje, J. *Organometallics* **1995**, *14*, 3081.

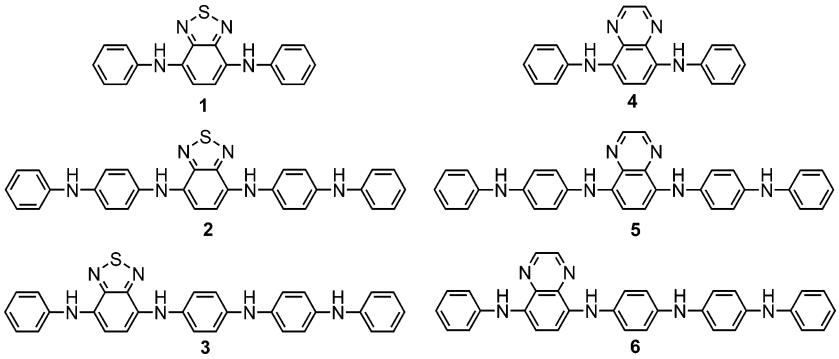

FIGURE 1. *p*-Phenylenediamine derivatives bearing a benzothiadiazole (**1**−**3**) or quinoxaline (**4**−**6**) unit.

SCHEME 2. Synthesis of Benzothiadiazoles 1−3[a]

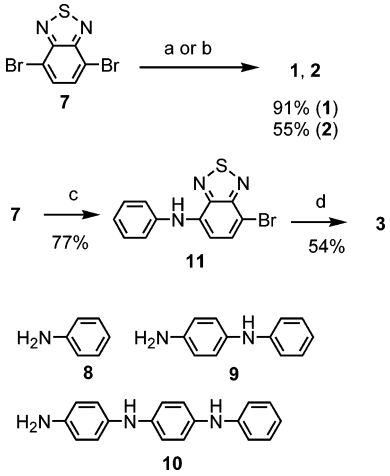

[a] Reagents and conditions: (a) 10 mol % $Pd(OAc)_2$, 11 mol % DPEphos, 280 mol % *t*-BuONa, 200 mol % **8**, toluene, reflux, 27 h. (b) 10 mol % $Pd(OAc)_2$, 11 mol % DPEphos, 280 mol % *t*-BuONa, 200 mol % **9**, toluene, reflux, 72 h. (c) 5 mol % $Pd(OAc)_2$, 5.5 mol % DPEphos, 140 mol % *t*-BuONa, 100 mol % **8**, toluene, reflux, 20 h. (d) 5 mol % $Pd(OAc)_2$, 5.5 mol % DPEphos, 140 mol % *t*-BuONa, 100 mol % **10**, toluene, reflux, 72 h.

SCHEME 3. Synthesis of Quinoxalines 4−6 from 5,8-Dibromoquinoxaline (Method A)[a]

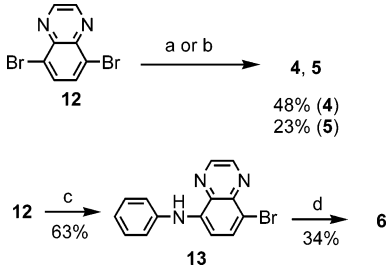

[a] Reagents and conditions: (a) 10 mol % $Pd(OAc)_2$, 11 mol % BINAP, 280 mol % *t*-BuONa, 200 mol % **8**, toluene, reflux, 72 h. (b) 10 mol % $Pd(OAc)_2$, 11 mol % BINAP, 280 mol % *t*-BuONa, 200 mol % **9**, toluene, reflux, 72 h. (c) 5 mol % $Pd(OAc)_2$, 5.5 mol % BINAP, 140 mol % *t*-BuONa, 100 mol % **8**, toluene, reflux, 16 h. (d) 5 mol % $Pd(OAc)_2$, 5.5 mol % DPEphos, 140 mol % *t*-BuONa, 100 mol % **10**, toluene, reflux, 72 h.

SCHEME 4. Transformation from Benzothiadiazoles to Quinoxalines (Method B)[a]

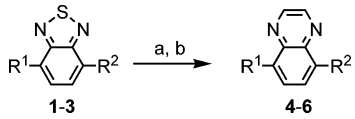

[a] Reagents and conditions: (a) 900 mol % zinc powder, AcOH, 70 °C, 3 h. (b) 120 mol % glyoxal, EtOH−H_2O, rt, 6 h.

metrical derivative **3**, the amination of **7** with an equimolar amount of **8** was performed at 80 °C to give the monocoupled product **11** selectively, followed by the coupling with the aniline trimer **10**.

Quinoxaline derivatives **4**−**6** were synthesized via two routes (methods A and B). Method A is based on the palladium-catalyzed amination of 5,8-dibromoquinoxaline (**12**)[25] in the presence of BINAP or DPEphos as a ligand (Scheme 3). Benzothiadiazole derivatives **1**−**3** could be transformed to the corresponding quinoxalines **4**−**6**, respectively. As shown in Scheme 4 (method B), reduction of **1** with zinc powder gave the corresponding *o*-phenylenediamine derivative, followed by the condensation with glyoxal to afford **4** in 39% yield. The preparation of **5** and **6** was also carried out under similar conditions.

^{1}H NMR of **1**−**6** indicates that hydrogen bonding exists between the imine nitrogen on the benzothiadiazole or quinoxaline ring and the amine adjacent to the heterocycle. Chemical shifts of the N−H apart from the BT/QX ring ranges from 5.6 to 5.8 ppm, whereas an approximately 1 ppm lower-field shift was observed with the N−H attached to the BT/QX ring (Figure 2).

2. X-ray Crystal Structure. Further structural information of **2** and **5** was obtained by X-ray crystallography, as shown in Figures 3 and 4, respectively. As for the structure of **2**·H_2O, the sums of angles at the amine nitrogen atoms are 359.5° (N2), 359.6° (N3), 359.1° (N12), and 359.9° (N13), respectively, supporting that they possess sp^3 hybrid structures. The dihedral angles of N1−C1−C2−N2 and N11−C101−C102−N12 are 5.4° and −1.8°, respectively. H1 and H3 are faced on the BT nitrogens. The distances of N1−H1, N2−H1, N11−H3, and N12−H3 are 2.42, 0.95, 2.67, and 0.92 Å, respectively. The angles of N2−C2−C1 and N12−C102−C101 are 115.9° and 117.4°, respectively, smaller than those of N2−C2−C3 and N12−C102−C103 (128.0° and 126.6°). These data indicate that hydrogen bonding exists between the imine nitrogen of the BT ring and the amine adjacent to the heterocycle. Aromatic rings are twisted against each other. The steric interaction between the hydrogen atom at C3 and the hydrogen atom at C5,

(25) (a) Tsubata, Y.; Suzuki, T.; Miyashi, T.; Yamashita, Y. *J. Org. Chem.* **1992**, *57*, 6749. (b) Yamamoto, T.; Sugiyama, K.; Kushida, T.; Inoue, T.; Kanbara, T. *J. Am. Chem. Soc.* **1996**, *118*, 3930.

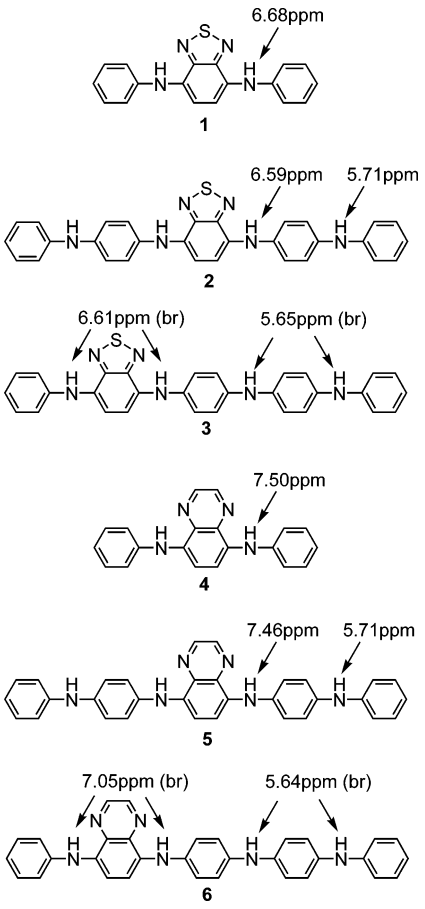

FIGURE 2. ^{1}H NMR chemical shifts of the N-H's.

however, causes the phenylene ring to rotate away from this orientation, resulting in a conformation with a dihedral angle of 50.7° between the BT ring and the adjacent phenylene. The dihedral angle between the phenylene and the terminal phenyl ring is 47.5°. Two molecules are present in a face-to-face manner with an interplanar distance of ca. 3.6 Å between the benzothiadiazole moieties, which form a π-stacked dimer in the crystal packing (see Supporting Information).

A similar structural feature was observed with **5**. The sums of angles around the amine nitrogen atoms are 358.4° (N2), 359.0° (N3), 359.9° (N12), and 353.5° (N13), respectively, showing their sp^3 hybrid structures. The dihedral angles of N1−C1−C2−N2, C1−C2−N2−H1, N11−C101−C102−N12, and C101−C102−N12−H3 are 1.3°, 9.9°, −1.3°, and −2.3°, respectively. H1 and H3 are faced on the QX nitrogens. The distances of N1−H1, N2−H1, N11−H3, and N12−H3 are 2.24, 0.91, 2.18, and 0.93 Å, respectively. The angles of N2−C2−C1 and N12−C102−C101 are 116.1° and 115.3°, respectively, smaller than those of N2−C2−C3 and N12−C102−C103 (127.1° and 128.1°, respectively). The dihedral angle between the QX ring and the adjacent phenylene is 29.9°. The dihedral angle between the phenylene and the terminal phenyl ring is 47.8°.

The hydrogen bondings of the BT and QX systems are significantly different. The length of the intramolecular hydrogen bond (N2−H1···N1) in the QX system is 2.23 Å, which is longer than 2.42 Å in the BT system. These data indicate that the strength of hydrogen bonding in the QX system is greater than that in the BT system. These data are in good agreement with the results observed in the solution state; in the NMR spectra, the chemical shift of N−H attached to the QX ring was shifted to lower field than that adjacent to the BT ring (Figure 2). The difference in the hydrogen bonding is considered to be partly due to the difference of the N lone pairs between BT/QX.

3. UV−vis Spectra. The absorption maxima of **1**−**6** in chloroform are shown in Table 1. The analogous compounds bearing pyrrolyl, thiophenyl, or phenyl moieties as a donor unit are also shown for comparison. The absorption maximum of **1** was 522 nm, exhibiting a HOMO−LUMO gap considerably smaller than that of thiophenyl **15** and phenyl analogues **16** and almost the same as that of the pyrrolyl analogue **14**, which is known to give the smallest HOMO−LUMO gap among these donor−acceptor compounds. Furthermore, longer wavelength absorption maximum was observed with **2** and **3** at 550 and 546 nm, respectively. Like in the BT systems, QX derivatives **4**−**6** also exhibited a smaller HOMO−

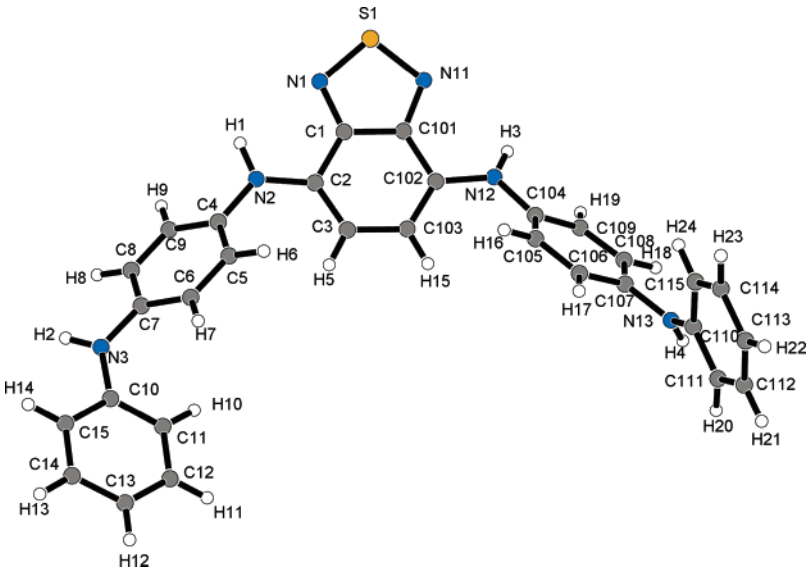

FIGURE 3. Molecular structure of **2**·H_2O.

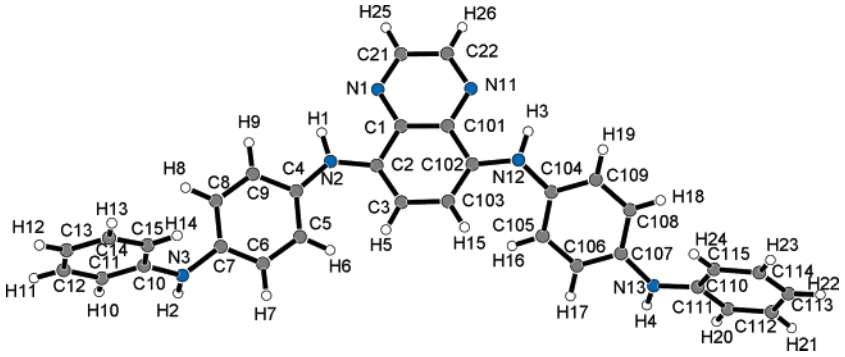

FIGURE 4. Molecular structure of **5**.

TABLE 1. Absorption Maxima of the Compounds 1−6 and 14−19

Compounds	1	2	3	4	5	6	14	15	16	17	18	19
λ_{max} (nm)	522	550	546	490	540	538	532	466	380	502	405	326

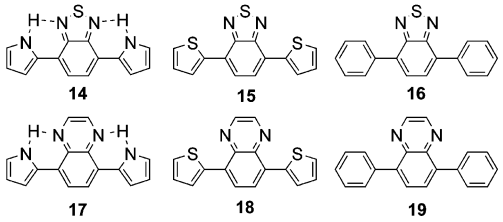

SCHEME 5. Plausible Redox Processes of 1

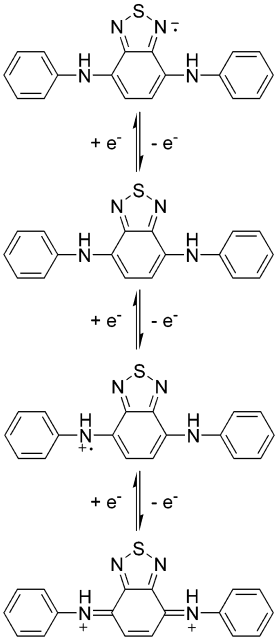

LUMO gap as compared with those of **18** and **19** and nearly the same as that of **17**. The absorption maxima of **5** and **6** were 540 and 538 nm, respectively. The intramolecular hydrogen bond might also play an important role to lower the HOMO−LUMO gap.

4. Electrochemical Properties. The redox behavior of **1**−**6** was investigated by cyclic voltammetry. The electrochemical behavior of **1** in acetonitrile may be explained by a redox process as shown in Scheme 5. A scan of **1** in acetonitrile from −2.2 to +1.2 V at 100 mV s^{-1} revealed two reversible one-electron oxidation processes at +0.10 and +0.44 V vs Fc/Fc^+ (Figure 5). The reduction wave indicates one-electron reduction process at −1.91 V. The QX derivative **4** showed similar electrochemical behavior with the redox potentials at −2.02, +0.06, and +0.45 V, respectively.

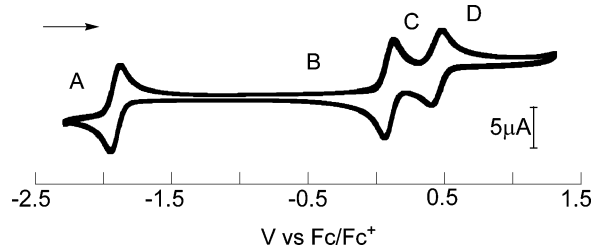

FIGURE 5. Cyclic voltammogram of **1** (1.0×10^{-3} M) in MeCN (0.10 M Bu_4NClO_4) at a platinum working electrode with scan rate = 100 mV s^{-1} under an argon atmosphere.

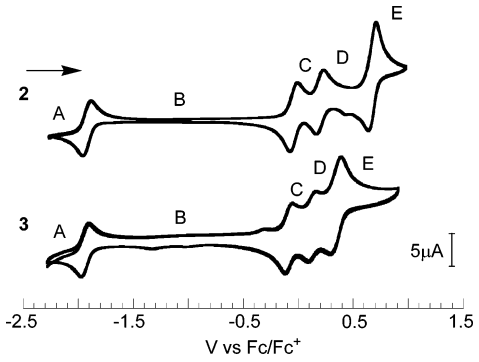

FIGURE 6. Cyclic voltammograms of **2** and **3** (1.0×10^{-3} M) in MeCN (0.10 M Bu_4NClO_4) at a platinum working electrode with scan rate = 100 mV s^{-1} under an argon atmosphere.

The results of cyclic voltammography of **2**, **3**, **5**, and **6** are shown in Scheme 6 and Figure 6. A scan from −2.2 to +1.4 V at 100 mV s^{-1} revealed three reversible one-electron redox processes and one two-electron process in every case. The first redox potential (E^1) is dependent on both the heterocyclic unit and its position. Unsymmetrical **3** is reduced into the radical anion at −1.95 V, which is 100 mV lower than for symmetrical **2** (−1.85 V), and **6** (−2.05 V) is also 110 mV more readily reduced than **5** (−1.94 V). An approximately 100 mV difference was observed between BT and QX derivatives. In contrast, the next two redox processes, B → C and C → D, are relatively independent of both the heterocyclic unit and its position. The BT/QX series **2/3** and **5/6** possess a similar second redox potential (E^2) and the difference

SCHEME 6. Plausible Redox Processes of the Pentamers

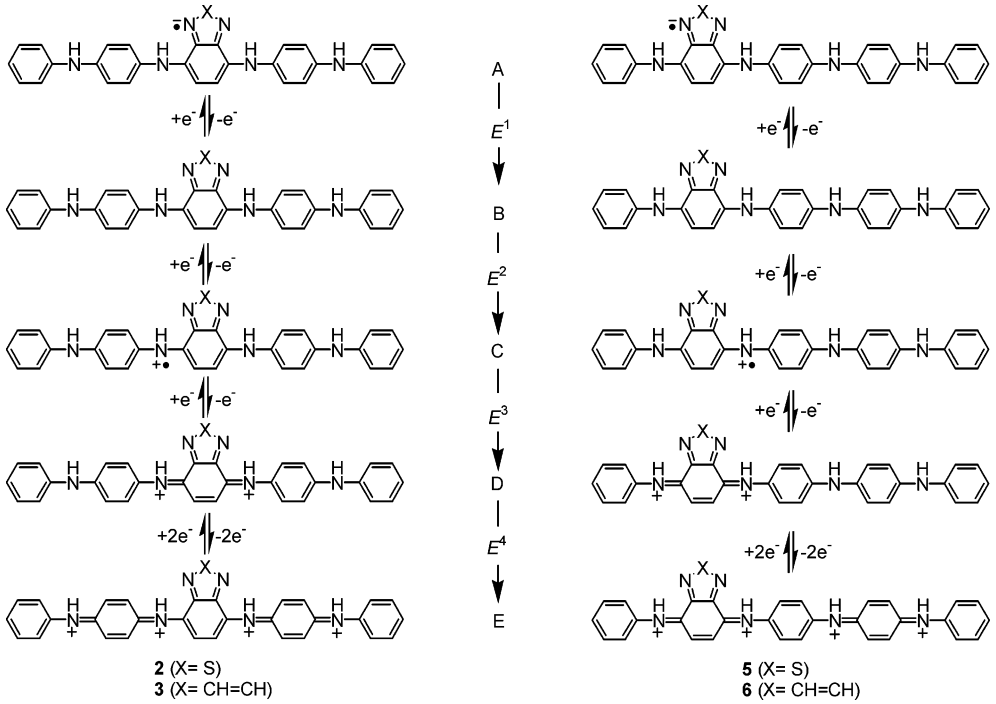

SCHEME 7. Chemical Oxidation of 1 and 4

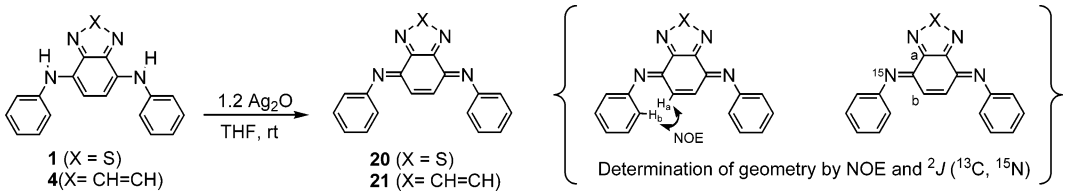

originated from the heterocycle BT/QX is only 30−40 mV (**2**: −0.09 V, **3**: −0.08 V) (**5**: −0.12 V, **6**: −0.12 V). The third redox potential (E^3) showed a slightly similar tendency to E^1, but the positional and heterocyclic difference is about 50 mV, which is apparently smaller than the difference in E^1. On the other hand, a distinct positional difference was observed in the two-electron redox process (D → E). The wave of **3** appeared at +0.35 V, which is much lower than that of **2** (+0.62 V). This oxidation corresponds to the formation of the fully oxidized form E. Such a lower E^4 may be due to the structure of the half-oxidized form D bearing the phenylenediamine moiety, where the next-HOMO lies.

5. Chemical Oxidation. Next, the chemical oxidation was investigated. When **1** was treated with 1.2 molar amounts of Ag_2O in THF, the (*E*,*E*)-quinonediimine derivative **20** was obtained quantitatively and no other isomers were detected (Scheme 7). The *E*,*E*-geometry was preliminarily determined by NOE, which was observed between H_a and H_b, and further confirmed by the coupling constant ^2J (^{13}C, ^{15}N).[26] The compound possessing ^{15}N-labeled quinonediimine nitrogens was prepared from $Ph^{15}NH_2$. The coupling constants of ^{15}N with C_a and C_b were measured as 7.46 and 2.71 Hz, respectively. This assignment is in good agreement with the NOE results. The same stereoisomer was selectively obtained in the oxidation of **4** and the geometry of **21** was also determined by NOE and ^2J (^{13}C, ^{15}N) ($^2J_{CaN}$ = 7,22 Hz, $^2J_{CbN}$ = 1.20 Hz). Such stereoselectivity might be induced by both kinetic and thermodynamic control. As stated in section 2, the starting reduced forms **1** and **4** favor the geometry in which H is faced on BT/QX and Ph locates away from BT/QX. Therefore, the oxidation may lead to the *E*,*E*-isomer under kinetic control. In addition, the *E*-geometry may also be favored thermodynamically due to the steric repulsion between the phenyl group and fused heterocycle.

Judging from their oxidation potentials, the behaviors of **2** and **3** in chemical oxidation are expected to be different. Oxidation of **2** with an equimolar amount of Ag_2O afforded a half-oxidized form **22**, which corresponds to D in the redox cycle shown in Scheme 6. Oxidation proceeded selectively at the BT position and **22** was isolated as one isomer, indicating that **22** also possesses the (*E*,*E*)-quinonediimine unit. Because of the high oxidation potential of **22**, no further oxidation proceeded even though an excess amount of Ag_2O was added under similar conditions. On the other hand, the fully oxidized form of **3** (**24**) is considered to be obtained with ease due to the low oxidation potential. Actually, **3** was oxidized with an equimolar amount of Ag_2O to give **23**, which was further converted to **24** quantitatively by treatment with another equimolar amount of Ag_2O (Scheme 8). It is noteworthy that **23** was also isolated as one stereoisomer,

(26) Kalinowski, H.-O.; Berger, S.; Braun, S. In *Carbon-13 NMR Spectroscopy*; Wiley: Chichester, 1998; p 572.

SCHEME 8. Chemical Oxidation of 2, 3, 5, and 6

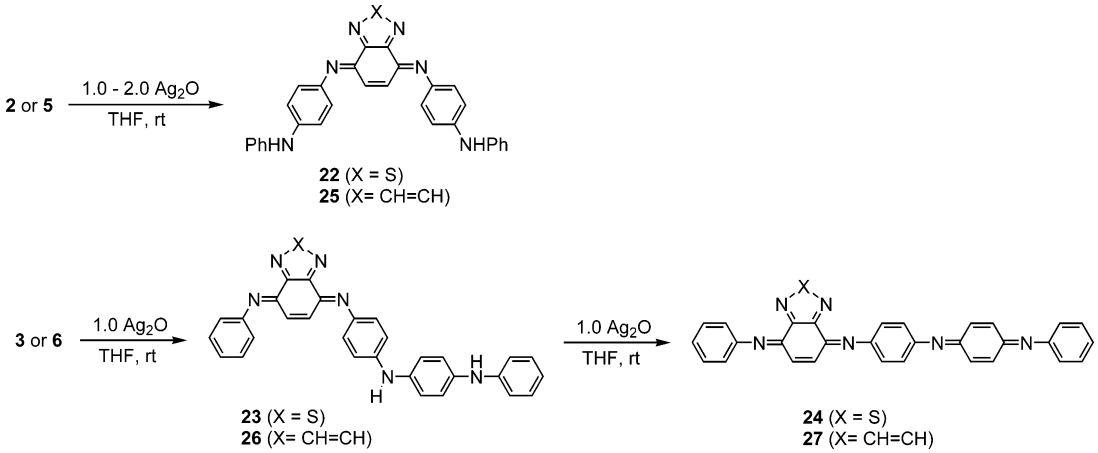

SCHEME 9. Chemical Oxidation of B3N2 and B5N4

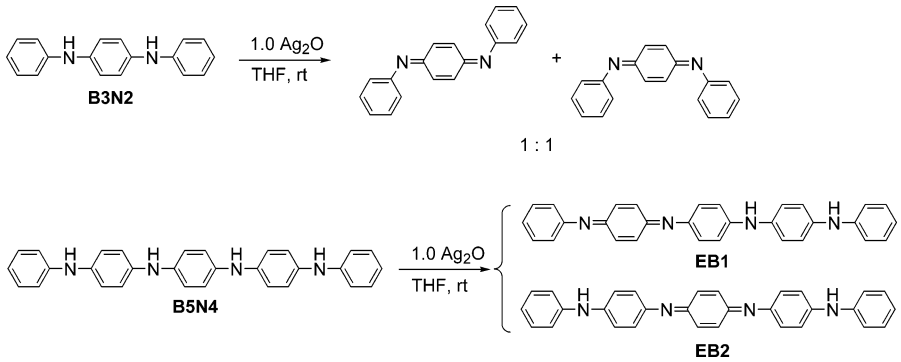

while **24** was obtained as a mixture of the stereoisomers and was very susceptible to moisture. Similar behavior should be expected in the oxidation of QX derivatives **5** and **6**. Unfortunately, control of mono- or dioxidation was difficult using Ag_2O as an oxidant and isolation of pure **25**, **26**, or **27** failed. This is partly because the third oxidation potentials of **5** and **6** are not so different as compared with those of BT derivatives. Further optimization of oxidation conditions should be required to isolate them.

There are two distinctive features in the chemical oxidation of the benzothiadiazole and quinoxaline derivatives as compared with the unsubstituted aniline oligomers (B3N2 and B5N4). One is that the initial oxidation selectively occurs at the heterocyclic position and the other is that the configuration of the quinonediimine on the BT/QX is *E,E*-geometry. This selectivity provides a uniform oxidized product (EB stage) and makes their chemical/physical properties tunable. In general, B3N2 is oxidized to yield a 1:1 isomeric mixture, and the oxidation of B5N4 affords a mixture of EB1 and EB2 (Scheme 9).[27] On the contrary, positional isomers **22** and **23** are independently prepared in the BT system and the comparison suggests important information on the properties of such heterocycle-hybridized polyaniline systems. In addition, it should be pointed out that *E,E*-configuration on BT/QX provides the bidentate coordination sites for transition metals. It has been reported by us[12] and other groups[28,29] that the hybrid systems of synthetic metals and transition metals are of potential as novel catalysts and materials. The BT/QX system is expected to develop a rational design for hybrid systems with transition metals. Their complexation behaviors will be described elsewhere.

The UV−vis spectra of **23** and **24** in acetonitrile were investigated (Figure 7). The absorption maximum of **23** is 560 nm, exhibiting a HOMO−LUMO gap smaller than that of **3** (546 nm). The absorption maximum of the fully oxidized form **24** (500 nm) was observed at a shorter wavelength compared to that of **3**. This behavior is similar to the feature as observed with ordinary polyaniline, i.e., the half-oxidized form (EB in Scheme 1) shows red-shifted maximum and the fully oxidized form (PE) shows blue-shifted maximum.[30]

The electrochemical properties of the half-oxidized forms **22**/**23** were also investigated. The cyclic voltammograms of **22** and **23** are shown in Figure 8. The redox potentials and calculated energy data are listed in Table 2. The first reversible redox waves at −2.04 V for **22** and −2.08 V for **23** are assigned to the one-electron reduction

(27) The related paper has been reported. See: MacDiarmid, A. G.; Zhou, Y.; Feng, J. *Synth. Met.* **1999**, *100*, 131.

(28) (a) Pickup, P. G. *J. Mater. Chem*. **1999**, *9*, 1641. (b) Kokil, A.; Shiyanovskaya, I.; Singer, K. D.; Weder, C. *J. Am. Chem. Soc.* **2002**, *124*, 9978. (c) Kokil, A.; Huber, C.; Caseri, W. R.; Weder, C. *Macromol. Chem. Phys*. **2003**, *204*, 40. (d) Wang, F.; Lai, Y.-H.; Han, M. Y. *Org. Lett*. **2003**, *5*, 4791 and references therein.

(29) (a) Kowalski, G.; Pielichowski, J. *Synlett* **2002**, 2107. (b) Kowalski, G.; Pielichowski, J.; Jasieniak, M. *Appl. Catal., A* **2003**, *247*, 295.

(30) Albuquerque, J. E.; Mattoso, L. H. C.; Balogh, D. T.; Faria, R. M.; Masters, J. G.; MacDiarmid, A. G. *Synth. Met.* **2000**, *113*, 19.

TABLE 2. UV−vis Spectra and Electrochemical Data in MeCN for 1−6, 22, and 23

	compound							
	1	**2**	**3**	**4**	**5**	**6**	**22**	**23**
λ_{max} (nm)	522	550	546	492	540	540	548	560
(eV)	2.37	2.25	2.27	2.52	2.30	2.30	2.26	2.21
E^1 (V)	−1.91	−1.85	−1.95	−2.02	−1.94	−2.05	−2.04	−2.08
E^2 (V)	+0.10	−0.09	−0.08	+0.06	−0.12	−0.12	−1.58	−1.67
E^3 (V)	+0.44	+0.18	+0.13	+0.45	+0.13	+0.07	−1.38	−1.38
E^4 (V)		+0.62	+0.35		+0.57	+0.44	+0.16	+0.03
E^5 (V)							+0.32	+0.31

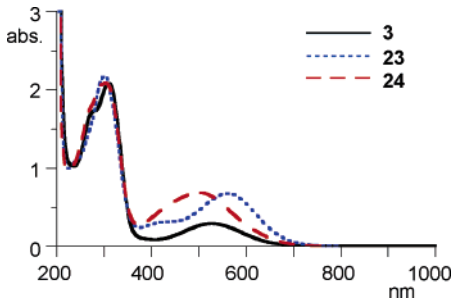

FIGURE 7. UV−vis spectra in MeCN (0.05 mM) of **3**, **23**, and **24** under an argon atmosphere.

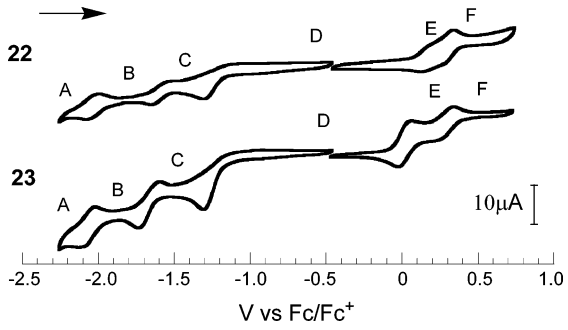

FIGURE 8. Cyclic voltammograms of **22** and **23** (1.0×10^{-3} M) in MeCN (0.1 M Bu_4NClO_4) at a platinum working electrode with scan rate = 100 mV s^{-1} under an argon atmosphere.

of the thiadiazole moiety as observed with **2** and **3**. The pseudoreversible redox waves at −1.58 and −1.38 V for **22** are assignable to the reduction of the quinonediimine moiety, while the waves for **23** were observed at −1.67 and −1.38 V. The fourth redox potential (E^4) is dependent on the position of the BT unit. Unsymmetrical **23** was 130 mV more readily oxidized than the symmetrical **22**. This behavior might be consistent with the difference in the fourth redox potential (E^4) of **2/3**. Interestingly, the redox waves corresponding to the formation of the fully oxidized form were observed as two waves of the one-electron process on **22/23** (E^4 and E^5), despite one wave of two-electrons process for **2/3** (E^4). The HOMO−LUMO gap of **23** is smaller than that of **22**, which is in good agreement with the results of their absorption maxima in the UV−vis spectra.

Conclusion

In summary, we have established the synthesis of *p*-phenylenediamine derivatives bearing a benzothiadiazole or quinoxaline unit, in which a small HOMO−LUMO gap system was attained. Cyclic voltammography indicated that the electrochemical properties depend on the chain length and the position of the heterocyclic unit. Chemical oxidation afforded only (*E*,*E*)-quinonediimine derivatives. The UV−vis spectra showed a similar feature as observed with ordinary polyaniline, i.e., the half-oxidized form showed a red-shifted maximum and the fully oxidized form showed a blue-shifted maximum. Large positional effect on the spectroscopic and electrochemical properties was observed in both reduced forms **2/3** and half-oxidized forms **22/23**. The present information may permit the design of novel aniline-heterocycle conjugate polymers.

Experimental Section

Compound 1. Compound **7** (294 mg, 1.0 mmol), $Pd(OAc)_2$ (23 mg, 0.1 mmol), DPEPhos (54 mg, 0.1 mmol), and *t*-BuONa (269 mg, 2.8 mmol) were mixed in toluene (5 mL). Aniline (218 μL, 2.4 mmol) was added dropwise to the solution, which was refluxed for 27 h. The reaction mixture was cooled and filtered through Celite. The Celite was rinsed with toluene and the mixture solution was concentrated. Purification by column chromatography (10% of CH_2Cl_2/hexane) gave **1** as a wine-red solid (289 mg, 91%).

Compound 2. Compound **7** (294 mg, 1,0 mmol), *N*-phenyl-1,4-phenylenediamine (405 mg, 2.2 mmol), $Pd(OAc)_2$ (23 mg, 0.1 mmol), DPEPhos (54 mg, 0.1 mmol), and *t*-BuONa (269 mg, 2.8 mmol) were mixed in toluene (5 mL). The reaction mixture was refluxed for 72 h. The mixture was cooled and filtered through Celite. The Celite was rinsed with toluene and the mixture solution was concentrated. Purification by column chromatography (50% of CH_2Cl_2/hexane) gave **2** as a dark blue solid (275 mg, 55%).

Compound 11. Compound **7** (294 mg, 1.0 mmol), $Pd(OAc)_2$ (11.5 mg, 0.05 mmol), DPEPhos (27 mg, 0.05 mmol), and *t*-BuONa (135 mg, 1.4 mmol) were mixed in toluene (5 mL). Aniline (109 μL, 1.2 mmol) was added dropwise to the solution, and the reaction mixture was stirred at 80 °C for 20 h. The reaction mixture was cooled and filtered through Celite. The Celite was rinsed with toluene and the mixture solution was concentrated. Purification by column chromatography (hexane) gave **11** as a yellow solid (236 mg, 77%).

Compound 3. 4-(4′-Aminophenyl)aminodiphenylamine (138 mg, 0.5 mmol), **11** (184 mg, 0.6 mmol), $Pd(OAc)_2$ (5.6 mg, 0.025 mmol), DPEPhos (15.3 mg, 0.028 mmol), and *t*-BuONa (67.3 mg, 0.7 mmol) were mixed in toluene (5 mL). The reaction mixture was refluxed for 72 h. The mixture was cooled and filtered through Celite. The Celite was rinsed with toluene and the mixture solution was concentrated. Purification by column chromatography (CH_2Cl_2) gave **3** as a violet solid (137 mg, 54%).

Compound 4 (by Method A). Compound **12** (288 mg, 1.0 mmol), $Pd(OAc)_2$ (23 mg, 0.1 mmol), BINAP (62 mg, 0.1 mmol), and *t*-BuONa (269 mg, 2.8 mmol) were mixed in toluene (10 mL). Aniline (218 μL, 2.4 mmol) was added dropwise to the solution, which was refluxed for 72 h. The reaction mixture was cooled and filtered through Celite. The Celite was rinsed with toluene and the mixture solution was concentrated.

Purification by column chromatography (30% of CH_2Cl_2/hexane) gave **4** as a wine-red solid (150 mg, 48%).

Compound 4 (by Method B). To a suspension of **1** (318 mg, 1.0 mmol) in a mixture solution of acetic acid (4.0 mL) and deionized water (1.5 mL) was added zinc powder (970 mg, 15 mmol) at 60 °C. The mixture was stirred for 12 h at 70 °C, filtered while hot, and trapped into 50% w/w of sodium hydroxide aqueous. After being cooled in the ice bath, the mixture was extracted with ether. The organic phase was washed with brine and dried over Na_2SO_4. Evaporation of the solvent gave the corresponding *o*-phenylenediamine derivative as a pale red solid. Without other purification, ethanol (30 mL) and then an aqueous solution of glyoxal (40%, 147 mg, 1.0 mmol) were added dropwise. The mixture was heated to reflux for 16 h and cooled. The mixture solution was concentrated. Purification by column chromatography (30% of CH_2Cl_2/hexane) gave **4** as a red-wine solid (112 mg, 39%).

Compound 5 (by Method A). Compound **12** (288 mg, 1,0 mmol), *N*-phenyl-1,4-phenylenediamine (405 mg, 2.2 mmol), $Pd(OAc)_2$ (23 mg, 0.1 mmol), BINAP (62 mg, 0.1 mmol), and *t*-BuONa (269 mg, 2.8 mmol) were mixed in toluene (10 mL). The reaction mixture was refluxed for 72 h. The mixture was cooled and filtered through Celite. The Celite was rinsed with toluene and the mixture solution was concentrated. Purification by column chromatography (50% of CH_2Cl_2/Hex) gave **5** as a dark blue solid (114 mg, 23%).

Compound 5 (by Method B). To a suspension of **2** (250 mg, 0.5 mmol) in a mixture solution of acetic acid (4.0 mL) and deionized water (1.5 mL) was added zinc powder (485 mg, 7.5 mmol) at 60 °C. The mixture was stirred for 12 h at 70 °C, filtered while hot, and trapped into 50% w/w of sodium hydroxide aqueous. After being cooled in the ice bath, the mixture was extracted with ether. The organic phase was washed with brine and dried over Na_2SO_4. Evaporation of the solvent gave the corresponding *o*-phenylenediamine derivative as a pale blue solid. Without other purification, ethanol (30 mL) and then an aqueous solution of glyoxal (40%, 73.5 mg, 0.5 mmol) were added dropwise. The mixture was heated to reflux for 16 h and cooled. The mixture solution was concentrated. Purification by column chromatography (50% of CH_2Cl_2/hexane) gave **5** as a dark blue solid (42 mg, 17%).

Compound 13. Compound **12** (288 mg, 1.0 mmol), $Pd(OAc)_2$ (23 mg, 0.1 mmol), BINAP (62 mg, 0.1 mmol), and *t*-BuONa (269 mg, 2.8 mmol) were mixed in toluene (5 mL). Aniline (218 μL, 2.4 mmol) was added dropwise to the solution, and the reaction mixture was stirred for 16 h at 80 °C. The reaction mixture was cooled and filtered through Celite. The Celite was rinsed with toluene and the mixture solution was concentrated. Purification by column chromatography (hexane) gave **13** as an orange solid (174 mg, 63%).

Compound 6 (by Method A). 4-(4′-Aminophenyl)aminodiphenylamine (138 mg, 0.5 mmol), **13** (165 mg, 0.6 mmol), $Pd(OAc)_2$ (5.6 mg, 0.025 mmol), BINAP (17.4 mg, 0.028 mmol), and *t*-BuONa (67.3 mg, 0.7 mmol) were mixed in toluene (5 mL). The reaction mixture was refluxed for 72 h. The mixture was cooled and filtered through Celite. The Celite was rinsed with toluene and the mixture solution was concentrated. Purification by column chromatography (CH_2Cl_2) gave **6** as a violet solid (84 mg, 34%).

Compound 6 (by Method B). To a suspension of **3** (250 mg, 0.5 mmol) in a mixture solution of acetic acid (4.0 mL) and deionized water (1.5 mL) was added zinc powder (485 mg, 7.5 mmol) at 60 °C. The mixture was stirred for 12 h at 70 °C, filtered while hot, and trapped into 50% w/w of sodium hydroxide aqueous. After being cooled in the ice bath, the mixture was extracted with ether. The organic phase was washed with brine and dried over Na_2SO_4. Evaporation of the solvent gave the corresponding *o*-phenylenediamine derivative as a pale violet solid. Without other purification, ethanol (30 mL) and then an aqueous solution of glyoxal (40%, 73.5 mg, 0.5 mmol) were added dropwise. The mixture was heated to reflux for 16 h and cooled. The mixture solution was concentrated. Purification by column chromatography (CH_2Cl_2) gave **6** as a violet solid (27 mg, 11%).

Acknowledgment. The use of the facilities of the Analytical Center, Graduate School of Engineering, Osaka University is acknowledged. We thank Dr. Toshiyuki Moriuchi for the X-ray crystallography. We also thank Ms. Toshiko Muneishi for the help of NMR measurement. This work was partially supported by a Grant-in-Aid for Scientific Research on Priority Areas (no.13128206) from the Ministry of Education, Sports, Science and Technology, Japan.

Supporting Information Available: X-ray crystallographic data of **2** and **5** in CIF format and analytical and spectroscopic data of all compounds described in Experimental Section. This material is available free of charge via the Internet at http://pubs.acs.org.

JO048324J